Nonspherical charge distributions and electrostatic interactions in crystals

N. E. Christensen*
Max-Planck-Institut für Festkörperforschung, Heisenbergstrasse 1, D-7000 Stuttgart 80, Federal Republic of Germany
(Received 22 November 1983)

A computationally simple method of calculating nonspherical charge distributions in solids from linear-muffin-tin-orbital band-structure calculations is described. The charge distribution is described accurately in the region between muffin-tin spheres in terms of wave functions based on "pseudo-muffin-tin" orbitals. The nonsphericity inside the spheres as described by the same orbitals is less accurate. For several applications, however, this is not serious. The density can easily be expressed as a Fourier series, which is convenient for calculation of interactions. As an example of application the scheme is used to calculate multipole moments and electrostatic interactions between Wigner-Seitz cells in a monoatomic crystal.

I. INTRODUCTION

The linear-muffin-tin-orbital (LMTO) method[1] in the atomic spheres approximation[1] (ASA) has been applied successfully in numerous calculations of physical properties of solids (see Refs. 2 and 3 and references given there). This applies to accurate quantitative predictions of Fermi-surface properties, cohesive properties as well as trends through the Periodic Table. The LMTO offers, in addition to an efficient computational scheme, the possibility of a detailed physical picture of the formation of energy bands and the way they determine, for example, the cohesive properties. One advantage of the LMTO-ASA in such studies is that it applies potentials and charge densities that are spherically symmetric around the atomic sites. There are cases, however, where quantitative calculations cannot be performed with sufficient accuracy in the ASA, since the nonsphericity of the true charge distribution plays an important role. The calculation[4] of elastic shear constants is one example of such a case. Although the linear augmented plane wave[1] (LAPW) and LMTO schemes can be[5] extended to include the nonspherical charge self-consistently, it is for some applications sufficient to use the nonspherical distribution corresponding to the eigenvectors obtained in the last iteration of a self-consistency cycle in the ASA approximation. The electrostatic interactions that influence the elastic properties of a solid are mainly due to the nonspherical charge in the outer parts of the Wigner-Seitz cells. Therefore, for such uses, we will only need a scheme which describes the charge density properly in the region which in a muffin-tin model is referred to as the interstial region of space. The accuracy of the description of the nonsphericity inside the inscribed spheres (muffin-tin spheres) is less important. We use such an approximate model for the charge density in the calculation of the intercellular electrostatic interactions in the transition metals, when we calculate the elastic shear constants.[4,6] Since a similar approximation may be sufficiently accurate for other purposes, and because the scheme is considerably simpler than a fully self-consistent, nonspherical calculation, we shall in the present paper describe the model in some detail. The wave functions are given as linear combinations of Bloch sums of the muffin-tin orbitals[1] (MTO's). In the interstial region, the MTO's are identical to the "pseudo-MTO's."[1] The MTO's and the pseudo-MTO's match differentiably at the sphere (radius S). Knowing the eigenvectors of the LMTO calculation, we can then construct a nonspherical charge density in the interstial regime from the pseudo-MTO's. As an approximation, for which some corrections in fact easily could be introduced,[5,7] we assume that the *nonspherical part* of the distribution also *inside* the sphere can be represented by the pseudo-MTO's. This simplified description leads directly to a Fourier representation of the charge density which is convenient in calculation of electron interactions. The calculation of charge densities in this approximation is described in Sec. II. As an example of application of the model, we calculate in Sec. III cellular multipole moments used in calculations of intercellular electrostatic interactions.

II. PSEUDO-MTO DENSITIES

A. Fourier representation

The wave function of a state $\vec{k}$, energy E, is in the LMTO expressed as an expansion in terms of muffin-tin orbital Bloch sums:

$$\psi^{\vec{k}}(E,\vec{r})=\sum_L A_L^{\vec{k}}\chi_L^{\vec{k}}(\vec{r}) , \tag{1}$$

$$\chi_L^{\vec{k}}(\vec{r})=\sum_{\vec{R}} e^{i\vec{k}\cdot\vec{R}}\chi_L(\vec{r}-\vec{R}) . \tag{2}$$

The present description is restricted to monoatomic crystals. The index L is a short notation of the angular and azimuthal quantum numbers, (l,m), the vectors $\vec{R}$ are the real-space lattice vectors, and $\chi_L(\vec{r}-\vec{R})$ is a muffin-tin orbital centered at the position $\vec{R}$. A sketch of a muffin-tin orbital ($\phi\dot{\phi}$ augmented) is given in Fig. 1. This orbital coincides in the interstitial region, i.e., between the muffin-tin spheres, with the pseudo-MTO, $\tilde{\chi}_L$. The pseudo-MTO is a smooth function inside the spheres, derived[1] from a pseudopotential. At $r=S$, i.e., at the sphere,

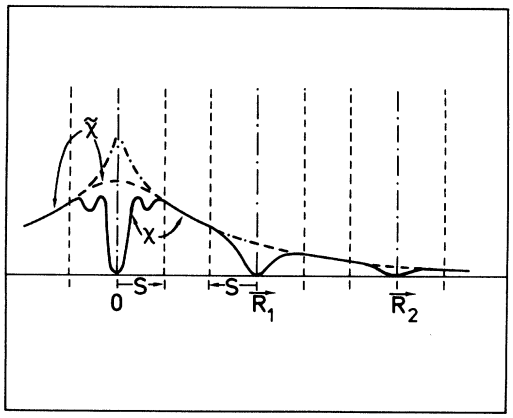

FIG. 1. Sketch of muffin-tin orbital ($\phi\dot{\phi}$ augmented) centered at the origin ($\vec{R}=0$) (solid line) and the pseudo-MTO (dashed line).

χ and $\tilde{\chi}$ match continuously and differentiably. We shall, in the following, need several expressions from Ref. 1. They will be referred to as LM, followed by the formula number in Ref. 1 [e.g., LM(4.14)].

A Bloch sum of pseudo-MTO's is

$$\tilde{\chi}_L^{\vec{k}}(\vec{r})=\sum_{\vec{R}} e^{i\vec{k}\cdot\vec{R}}\tilde{\chi}_L(\vec{r}-\vec{R}) \tag{3}$$

with [LM(4.14), LM(4.15)]

$$\tilde{\chi}_L^{\vec{k}}(\vec{r})=\chi_l(D_l)\sum_{\vec{G}} e^{i(\vec{k}+\vec{G})\cdot\vec{r}}F_L(\vec{k}+\vec{G}) \tag{4}$$

and

$$F_L(\vec{k}+\vec{G})=(2l+1)(2l+3)\frac{4\pi}{\Omega}\frac{j_{l+1}(|\vec{k}+\vec{G}|S)}{|\vec{k}+\vec{G}|^3}$$
$$\times Y_L(\vec{k}+\vec{G}) . \tag{5}$$

Here $j_l(x)$ is a spherical Bessel function, and $Y_L(\hat{K})$ a spherical harmonic, $Y_l^m(\hat{K})$. The normalization factor $\chi_l(D_l)$ is defined in Ref. 1 [LM(4.6), LM(2.13)]. A function $\Theta(\vec{r})$ is introduced as

$$\Theta(\vec{r})=\begin{cases}1 & \text{inside any muffin-tin sphere}\\ 0 & \text{elsewhere}\end{cases}$$

and in terms of this, we define the function

$$\chi'_L(\vec{r})=\tilde{\chi}_L(\vec{r})+[\chi_L(\vec{r})-\tilde{\chi}_L(\vec{r})]\Theta(\vec{r}) . \tag{6}$$

Since χ and $\tilde{\chi}$ coincide in the interstitial region, Eq. (6) is just a rewriting of the ("real") MTO.

The electron density associated with the state $(\vec{k},E)$ is

$$\rho_{\vec{k}}(\vec{r})=|\psi^{\vec{k}}(E,\vec{r})|^2=\sum_{L',L} A_{L'}^{\vec{k}*}A_L^{\vec{k}}\chi_{L'}^{\vec{k}*}(\vec{r})\chi_L^{\vec{k}}(\vec{r})$$
$$=\sum_{L',L} A_{L'}^{\vec{k}*}A_L^{\vec{k}}\chi'^{\vec{k}*}_{L'}\chi'^{\vec{k}}_{L} . \tag{7}$$

With the use of (6) we get

$$\rho_{\vec{k}}(\vec{r})=\sum_{L',L} A_{L'}^{\vec{k}*}A_L^{\vec{k}}[\tilde{\chi}_{L'}^{\vec{k}*}\tilde{\chi}_L^{\vec{k}}$$
$$+(\chi_{L'}^{\vec{k}*}\chi_L^{\vec{k}}-\tilde{\chi}_{L'}^{\vec{k}*}\tilde{\chi}_L^{\vec{k}})\Theta(\vec{r})] . \tag{8}$$

The A coefficients are the LMTO eigenvectors, the $A_{Lj}^{\vec{k}}$ in Ref. 1 (we have here suppressed the band indexing). The first term in Eq. (8) gives the nonspherical charge in the interstitial region. Inside the MT sphere ρ is given by the term due to the real MTO's (χ). The approximation which we will use here consists in replacing $(\chi\chi-\tilde{\chi}\tilde{\chi})$ *inside* the sphere by its *spherical average*, i.e., we replace (8) by

$$\rho_{\vec{k}}(\vec{r})\simeq\sum_{L',L} A_{L'}^{\vec{k}*}A_L\tilde{\chi}_{L'}^{\vec{k}*}(\vec{r})\tilde{\chi}_L^{\vec{k}}(\vec{r})$$
$$+\sum_{\vec{R}}[\rho_{\vec{k}}(|\vec{r}-\vec{R}|)-\tilde{\rho}_{\vec{k}}(|\vec{r}-\vec{R}|)]\Theta(\vec{r}) . \tag{9}$$

We have here assumed that the *nonsphericity* of the charge inside the spheres to sufficient accuracy can be described by the continuation from the sphere towards its center of the nonspherical part of the pseudo-MTO density. This approximation is most approximate for states of large l, since the radial part of the speudo-MTO's inside the sphere behave[1] as $\sim r^l$ and r^{l+2} (see Sec. II B). Although there are obvious ways to correct for these errors, we shall not do this here. The first term in (9) gives what we in the following will refer to as the *pseudodensity* $\tilde{\rho}$:

$$\tilde{\rho}_{\vec{k}}(E_{\vec{k}}^j,\vec{r})=\sum_{L',L} A_{L'j}^{\vec{k}*}A_{Lj}^{\vec{k}}\tilde{\chi}_{L'}^{\vec{k}*}(\vec{r})\tilde{\chi}_L^{\vec{k}}(\vec{r}) . \tag{10}$$

The total pseudodensity is obtained by summation over all occupied states:

$$\tilde{\rho}(\vec{r})=\sum_{\vec{k},j}^{\text{occ}}\tilde{\rho}_{\vec{k}}(E_{\vec{k}}^j,\vec{r}) . \tag{11}$$

The pseudodensity can conveniently be expressed as a Fourier sum:

$$\tilde{\rho}(\vec{r})=\sum_{\vec{G}}\tilde{\rho}_{\vec{G}}e^{i\vec{G}\cdot\vec{r}} , \tag{12a}$$

where

$$\tilde{\rho}_{\vec{G}}=\sum_{\vec{k},j}^{\text{occ}}\tilde{\rho}_{\vec{G}}^{\vec{k}}(E_{\vec{k}}^j) \tag{12b}$$

with

$$\tilde{\rho}_{\vec{G}}^{\vec{k}}(E_{\vec{k}}^j)=\frac{1}{\Omega}\int_\Omega\tilde{\rho}_{\vec{k}}(E_{\vec{k}}^j,\vec{r})e^{-i\vec{G}\cdot\vec{r}}d\vec{r} . \tag{12c}$$

The Fourier components (12c) can, by using (3) and (4), be expressed as

$$\tilde{\rho}_{\vec{G}}^{\vec{k}}(E_{\vec{k}}^j)=\sum_{L',L,\vec{G}'} A_{L'}^{\vec{k}*}A_L^{\vec{k}}F_{L'}^*(\vec{G}'+\vec{k})F_L(\vec{G}'+\vec{G}+\vec{k})$$
$$\times\chi_{l'}(D_{l'})\chi_l(D_l) . \tag{13}$$

The functions F do not depend on the actual crystal po-

tential. The products $F_L^* F_L$ can, once for a given structure, be summed internally over $\vec{G}'$, and stored on file together with the structure constants[1] and combined correction terms.[1] For the transition metals we[4] needed ~ 300 $\vec{G}$ vectors, and therefore, for a reasonable density of the k mesh, a substantial amount of data needs to be stored; but the fact that we only need to calculate these quantities once for a given structure compensates for the somewhat long computation times needed. It can easily be demonstrated that the $\tilde{\rho}_{\vec{G}}$ coefficients are real for crystals with inversion symmetry. The proper symmetry of $\rho(\vec{r})$, Eq. (12), is obtained by averaging $\tilde{\rho}_{\vec{G}}$ over the star of $\vec{G}$. The $|\vec{G}|$ convergence of $\tilde{\rho}_{\vec{G}}$ is illustrated in Fig. 2, showing the Fourier components in the case of Mo. Here as well as in the further numerical examples that will be shown, we, in addition to the approximation already mentioned, replace the muffin-tin radius by the atomic-sphere radius. A contour plot of the pseudodensity in Mo is shown in Fig. 3. The variations of the density in the outer part of the cell, for example, over the muffin-tin sphere, is of the same order of magnitude as the average density at the surface of the atomic sphere. This explains why the inclusion of nonsphericity is important[4,6] in the calculation of the elastic constants.

B. Spherical average

The present approximation describes the total electron density as [Eqs. (9)—(12)]

$$\rho(\vec{r})=\tilde{\rho}(\vec{r})+[\rho_{\mathrm{ASA}}-\langle\tilde{\rho}\rangle_{\mathrm{sph}}]\Theta(\vec{r}) , \tag{14}$$

where ρ_{ASA} is the usual, spherically-symmetric charge density used in the LMTO. Inside the (muffin-tin) spheres we need, in the calculation of $\rho(\vec{r})$ by (14), the difference between this and the spherical average $\langle\tilde{\rho}\rangle_{\mathrm{sph}}$ of the pseudodensity. The spherical average of the pseudodensity in the sphere at $\vec{R}=0$, can be calculated in two ways: (i) from a one-center expansion similar to LM(4.21) (but using pseudo-MTO's) or (ii) by averaging directly $\tilde{\rho}(\vec{r})$ given by (12). The latter calculation (ii) is easily performed by using the expansion of a plane wave in terms of spherical Bessel functions:

$$e^{i\vec{G}\cdot\vec{r}}=4\pi\sum_L i^l j_l(Gr)Y_L^*(\hat{G})Y_L(\hat{r}) . \tag{15}$$

Owing to the orthogonality of the spherical harmonics

$$\langle e^{i\vec{G}\cdot\vec{r}}\rangle_{\mathrm{sph}}=\sqrt{4\pi}j_0(Gr)Y_0^*(\hat{G})=j_0(Gr)$$

and

$$\langle\tilde{\rho}(\vec{r})\rangle_{\mathrm{sph}}=\sum_{\vec{G}}\tilde{\rho}_{\vec{G}}j_0(Gr) . \tag{16}$$

The other method, referred to as (i) above, employs a one-center expansion[1,5] of the pseudo-MTO Bloch sum. We choose for D_l in Eq. (4) the value $-l-1$, in which case $\chi_l(D_l)=\Phi(-l-1)\equiv\Phi_l(-)$; see LM(4.6) and LM(2.13). The one-center expansion of $\tilde{\chi}_L^{\vec{k}}(\vec{r})$ is

$$\tilde{\chi}_L^{\vec{k}}(\vec{r})=\frac{\Phi_l(-)}{\tilde{\Phi}_l^{(-)}}\sum_{L'}[\tilde{\phi}_{\nu L}(\vec{r})\tilde{\Pi}_{L'L}^{\vec{k}}+\dot{\tilde{\phi}}_{\nu L}(\vec{r})\tilde{\Omega}_{L'L}^{\vec{k}}] . \tag{17}$$

The radial parts, $\tilde{\phi}_{\nu l}(r)$ and $\dot{\tilde{\phi}}_{\nu l}(r)$, of $\tilde{\phi}_{\nu L}(\vec{r})$ and $\dot{\tilde{\phi}}_{\nu L}(\vec{r})$ are obtained from the requirement of normalization of $\tilde{\phi}$ and the orthogonality of $\tilde{\phi}$ and $\dot{\tilde{\phi}}$:

$$\tilde{\phi}_{\nu l}(r)=\left[\frac{(2l+3)}{S^3}\right]^{1/2}\left[\frac{r}{S}\right]^l , \tag{18}$$

$$\dot{\tilde{\phi}}_{\nu l}(r)=\tfrac{1}{2}\sqrt{(2l+3)S}\times\left[\frac{1}{2l+5}\left[\frac{r}{S}\right]^l-\frac{1}{2l+3}\left[\frac{r}{S}\right]^{l+2}\right] . \tag{19}$$

The elements of the $\tilde{\Omega}$ and $\tilde{\Pi}$ matrices are defined as in LM(4.21):

$$\tilde{\Pi}_{LL'}^{\vec{k}}=\delta_{LL'}-\frac{\tilde{T}_{LL'}^{\vec{k}}}{\tilde{\omega}_- -\tilde{\omega}_+} , \tag{20a}$$

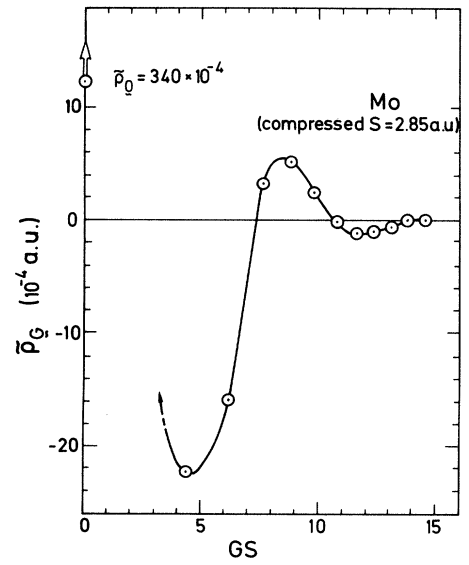

FIG. 2. Fourier components $\tilde{\rho}_{\vec{G}}$ of the pseudodensity for Mo as a function of GS.

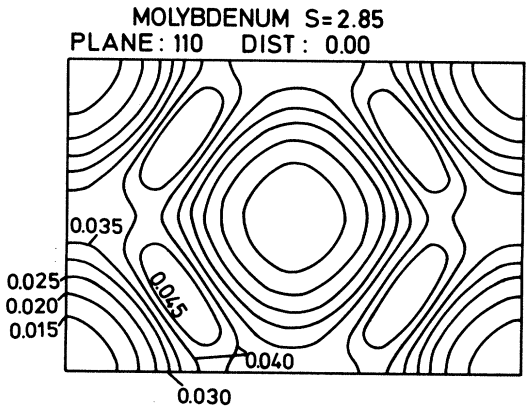

FIG. 3. Contour plot of the pseudo-MTO electron density in Mo in the (110) plane.

$$\tilde{\Omega}^{\vec{k}}_{LL'}=\tilde{\omega}_-\delta_{LL'}-\frac{\tilde{\omega}_+}{\tilde{\omega}_--\tilde{\omega}_+}\tilde{T}^{\vec{k}}_{LL'} . \tag{20b}$$

The free-electron potential parameters are given in Ref. 1,

$$\tilde{\omega}_+=0 , \tag{21a}$$

$$\tilde{\omega}_-=\frac{1}{2}\frac{(2l+1)(2l+5)}{S^2} , \tag{21b}$$

$$\tilde{\Phi}_l(-)=\frac{2l+5}{2(2l+3)^{1/2}}\frac{1}{S^{3/2}} , \tag{21c}$$

$$\tilde{\Phi}_l(+)=\tilde{\phi}_{\nu l}(S) . \tag{21d}$$

From (21a) it follows that $\tilde{\Omega}$ is diagonal,

$$\tilde{\Omega}^{\vec{k}}_{LL'}=\tilde{\omega}_-\delta_{LL'} . \tag{20b'}$$

The matrix $\tilde{T}$ is defined in analogy with LM(4.11).

In terms of the eigenvectors $\vec{A}^{\vec{k}}$, the spherical part of the pseudo-MTO density is, using

$$\tilde{\psi}^{\vec{k}}(E,\vec{r})=\sum_L A^{\vec{k}}_L\tilde{\chi}^{\vec{k}}_L(\vec{r})$$

with Eq. (17),

$$\langle\tilde{\rho}(\vec{r})\rangle_{\rm sph}=\tilde{\rho}_{\rm sph}(r)$$
$$=\sum_{\vec{k},L}^{\rm occ}[\,\tilde{\phi}^2_{\nu L}(r)\,|\,\vec{\alpha}^{\vec{k}}\,|^2+\dot{\tilde{\phi}}^2_{\nu L}(r)\,|\,\vec{\beta}^{\vec{k}}\,|^2$$
$$+2\tilde{\phi}_{\nu L}(r)\dot{\tilde{\phi}}_{\nu L}(r){\rm Re}(\vec{\beta}^{\vec{k}}\cdot\vec{\alpha}^{\vec{k}})] , \tag{22}$$

where the elements of the vectors $\vec{\alpha}^{\vec{k}}$ and $\vec{\beta}^{\vec{k}}$ are

$$\alpha^{\vec{k}}_{LL'}=\tilde{\Pi}^{\vec{k}}_{L'L}A^{\vec{k}}_{L'}\frac{\Phi_{l'}(-)}{\tilde{\Phi}_{l'}(-)} , \tag{22a}$$

$$\beta^{\vec{k}}_{LL'}=\tilde{\Omega}^{\vec{k}}_{L'L}A^{\vec{k}}_{L'}\frac{\Phi_{l'}(-)}{\tilde{\Phi}_{l'}(-)} . \tag{22b}$$

The spherical averages Eqs. (16) and (22) are in practical calculations (slightly) different. In Eq. (16) a finite number of $\vec{G}$ vectors are included, and in the LMTO a finite number of partial waves are used, i.e., the maximum value of l in (22) is finite (usually 2 or 3). For the calculation of the second term (in [ ] in Eq. (14)), the expression (22) should be used. This ensures that $\rho_{\rm ASA}$ and $\langle\tilde{\rho}\rangle_{\rm sph}$ are consistent with respect to l convergence. In Fig. 4 we compare, for Mo, the results obtained from Eq. (22) and Eq. (16), dashed and dotted curves, respectively. The spherical symmetric pseudodensities are further compared

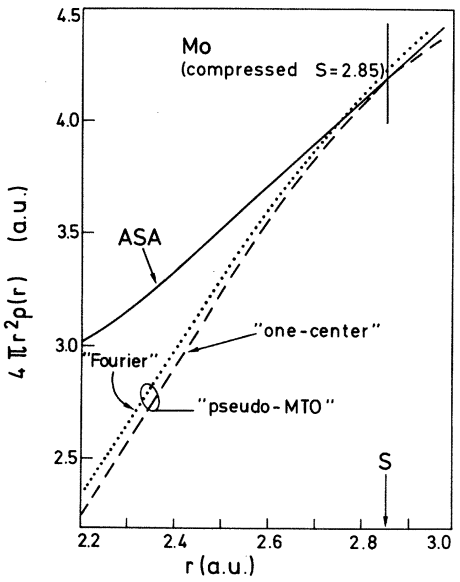

FIG. 4. Radial electron densities in Mo. Solid line: ASA valence density. Dashed line: spherical average of pseudo-MTO density from one-center expansion [Eq. (22)]. Dotted line: spherical average of pseudo-MTO density in Fourier representation [Eq. (16)].

to the "correct" spherically averaged valence-electron density (solid line). Passing from the sphere towards the interior, the deviations between the radial pseudodensities and the correct spherical density increase rapidly, as expected [Eqs. (18) and (19)].

III. EXAMPLE: MULTIPOLE MOMENTS

Although neutral, the Wigner-Seitz cells in a monoatomic solid interact electrostatically due to their nonspherical shape and due to the fact that they contain a non- spherical charge distribution. The interaction energy between a selected cell (at $\vec{R}=0$) and all the other cells can[8,9,5,6] be expressed as

$$U_{\rm el}=e^2\sum_{l,l',m,m'}B^{mm'}_{ll'}Q^m_l(Q^{m'}_{l'}S^{-m-m'}_{l+l'})^* \tag{23}$$

where

$$S^m_l=\sum_{\vec{R}\,(\neq\vec{0})}\frac{Y^m_l(\hat{R})}{R^{l+1}} \tag{24}$$

and[6,8,9]

$$B^{mm'}_{ll'}=\frac{2l+1}{4\pi}(-1)^{l'+m'}\left[4\pi\frac{(2l'+1)(l+l'+m'-m)!(l+l'-m'+m)!}{(2l+2l'+1)(2l+1)(l'+m')!(l'-m')!(l+m)!(l-m)!}\right]^{1/2} . \tag{25}$$

The multipole moments are obtained by integrating over the cell:

$$Q^m_l=\frac{4\pi}{2l+1}\int_{\rm cell\ \Omega}\rho(\vec{r})r^l Y^m_l(\hat{r})d\vec{r} . \tag{26}$$

It will be demonstrated here that the expressions (14) and (12) for the charge density allow a computationally quite simple calculation of the multipole moments [Eq. (26)]. Furthermore, those parts of a practical calculation which are particular time consuming can be made once and for all for a given structure, for example, fcc or bcc.

The Wigner-Seitz cell is neutral, i.e., the moment corre-

sponding to $l=0$ is 0. The second term in (14) is nonzero only inside the inscribed sphere, where it is spherically symmetric. This term does not contribute to the moments for $l>0$. The density described by Eq. (14) has tacitly been assumed to be due to the (occupied) band states. In order to obtain the total density we ought to add the core density to this. We shall here assume that this (spherically symmetric) density is 0 outside the muffin-tin sphere (if not, it is easy to include its contribution to Q_l^m). Thus only the pseudodensity $\tilde{\rho}(\vec{r})$ gives important contributions to Q_l^m.

From Eqs. (12) and (15) we have

$$Q_L = Q_l^m = \frac{(4\pi)^2}{2l+1} \sum_{\vec{G}} \tilde{\rho}_{\vec{G}} I_{\vec{G}}^L \ , \tag{27a}$$

where

$$I_{\vec{G}}^L = \sum_{L'} i^{l'} Y_{L'}^*(\hat{G}) \int_{\text{cell } \Omega} r^l j_{l'}(Gr) Y_{L'}(\hat{r}) Y_L(\hat{r}) d\vec{r} \ . \tag{27b}$$

This shows that the only part of the calculation that requires some computational effort, $I_{\vec{G}}^L$, can be calculated once and for all for a given structure. The actual crystal potential enters via $\tilde{\rho}_G$ in (27a) only. Furthermore, the application of symmetry-adapted angular momentum functions greatly reduces the amount of practical computation. In the cubic cases, Kubic harmonics, K_l^n are used instead of the spherical harmonics. This means that, in analogy with (27b), we must calculate integrals of the type

$$\Gamma_{ll'}^{nn'}(G) = \int_{\text{cell } \Omega} r^l j_{l'}(Gr) K_{l'}^{n'}(\hat{r}) K_l^n(\hat{r}) d\vec{r} \ . \tag{28}$$

The Kubic harmonics are nonzero only for $l=4$, $6,8,10,12,14,\ldots$, and for $l=4$, $6,8,10$ only one K_l^n exists for each l. For $l=12$, n takes two values. The cellular integration of a product of Y_L functions (or K_L^n) and a spherical symmetric function $f(r)$ can, for example, be performed by means of the application of "theta operators"[10]

$$T \equiv \int_{\text{cell}} f(r) Y_l^m(\hat{r}) Y_{l'}^{m'}(\hat{r}) d\vec{r} = \int_0^R r^2 f(r) \Theta_{ll'}^{mm'}(r) dr \ , \tag{29}$$

where R is larger than (or equal to) the radius of the circumscribed sphere. The theta operators are

$$\Theta_{ll'}^{mm'}(r) = \int_{\text{sphere}(r) \in \text{cell}} Y_l^m(\hat{r}) Y_{l'}^{m'}(\hat{r}) d\hat{r} \ . \tag{30}$$

The integral is over that part of the surface of the sphere with radius r which lies inside the cell. The Θ operators can be calculated once and for all for a given structure, for example, by means of a tetrahedron[11] integration scheme. In order to reduce numerical errors it is preferable, instead of the theta operators to use integrated operators $u_{ll'}^{mm'}(r)$. Partial integration in (29) gives

$$\int_0^R f(r) r^2 \Theta_{ll'}^{mm'}(r) dr = [f(r) u_{ll'}^{mm'}(r)]_0^R - \int_0^R f'(r) u_{ll'}^{mm'}(r) dr \ , \tag{31}$$

where

$$u_{ll'}^{mm'}(r) = \int_0^r r^2 \Theta_{ll'}^{mm'}(r') dr' = \int_{\text{cell} \in \text{sphere}(r)} Y_l^m(\hat{r}') Y_{l'}^{m'}(\hat{r}') d\vec{r}' \ . \tag{32}$$

The volume integral in (32) is over that part of the cell which lies inside the sphere of radius r. Separating the contributions from the inscribed sphere, the u operator is

$$u_{ll'}^{mm'}(r) = \begin{cases} \delta_{ll'} \delta_{mm'} \dfrac{r^3}{3} & \text{for } r \le R_1 \\ \delta_{ll'} \delta_{mm'} \dfrac{R_1^3}{3} + \displaystyle\int_{\substack{R_1 \le |\vec{r}'| \le r, \\ \vec{r}' \in \text{cell}}} Y_l^m(\hat{r}') Y_{l'}^{m'}(\hat{r}') d\vec{r}' & \text{for } r > R_1 \end{cases} \tag{33}$$

where R_1 is the inscribed sphere radius. In the calculation of shear constants[4,6] we needed to perform integration of cells of sheared lattices. Since we did not apply the tetrahedron method in these cases, but less accurate Monte Carlo integrations, the integral representation (31)—(33) was prefered.

As a numerical example, we show in Fig. 5 the moments

$$q_l = \frac{4\pi}{2l+1} \int_{\text{cell}} \tilde{\rho}(\vec{r}) r^l K_l(\hat{r}) d\vec{r} \tag{34}$$

for Pd (the two contributions for $l=12$ have been added). Although the moments decrease fast with l, at least $l=12$ must be included in energy calculations. This follows from Ref. 4 and from the calculated energies versus $l_{\max}$ shown in Fig. 6. The points in Fig. 6 which are connected by dashed lines were obtained from a muffin-tin charge density, i.e., only the *shape* of the cell influences the moments. The points connected with a full line represent calculations where the nonsphericity of the charge was taken into account. This nonsphericity influences the interaction energy as follows from Fig. 6 and it was found[4]

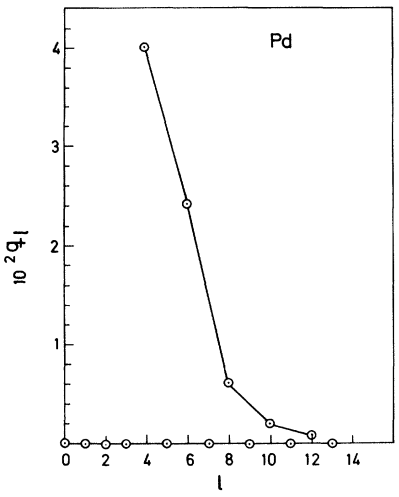

FIG. 5. Multipole moments for Pd [Eq. (34)]. Atomic units. Furthermore, q has been multiplied by $(2/a)^{l+3}$, a being the lattice constant.

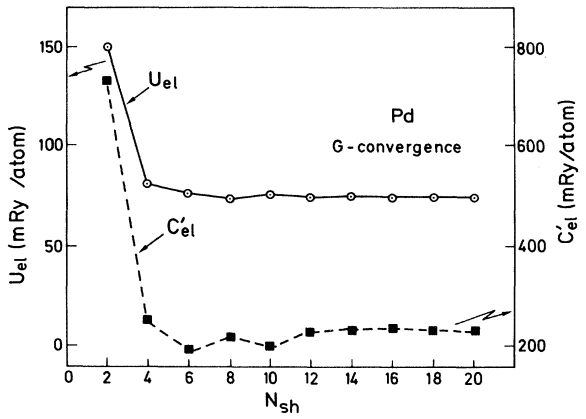

FIG. 7. G convergence of interaction energy [Eqs. (23), (26), and (27)]. N_{sh} is the number of "shells" included in the $\vec{G}$ summation. Moments with l up to $l=12$ included. In addition, the electrostatic contribution, c'_{el}, to the tetragonal elastic shear constant (Ref. 4) is shown.

to be very important in the calculation of the elastic shear constants. The interaction energy converges rapidly on $|\vec{G}|$. This is illustrated in Fig. 7, where the calculated values of U_{el} are shown as a function of the number of *G shells* included in the reciprocal-space summation.

IV. CONCLUSIONS

An approximate method for calculating the nonspherical charge density in a solid from LMTO band calculations has been described. The method leads to computationally simple expressions and those quantities which require most numerical calculation effort can, for a given structure, be calculated once for all. The Fourier representation of the density, which is obtained from the pseudo-MTO's, is calculated from quantities (F) which are essentially already included in computer codes which use the so-called combined correction term.[1] The Fourier representation is convenient in calculations of electron-electron interactions and is currently being implemented in total-energy calculations.[12] It is not yet clear whether our approximate treatment of the nonsphericity inside the spheres is sufficiently good for such calculations. The calculation of the multipole interactions is simple in the present scheme. In the calculation of the shear elastic constants[4] we needed to calculate the shear derivatives of the multipole moments. This was done in the scheme presented here, taking into account the proper shape of the Wigner-Seitz cells of the sheared lattice and shear deformation of the nonspherical charge. The latter contribution was calculated by changing the $\vec{G}$ vectors in the Fourier expansion according to the shear and keeping the $\tilde{\rho}_{\vec{G}}$ coefficients unchanged. In this way the sheared moments could be expressed in terms of band-structure quantities derived for the *unsheared* crystal and purely geometrical terms. Although the present model has been successful in some applications, its limitations have not yet been fully examined. The need of a better description of the nonsphericity inside the muffin-tin spheres[7] may be more urgent in cases different from those discussed here.

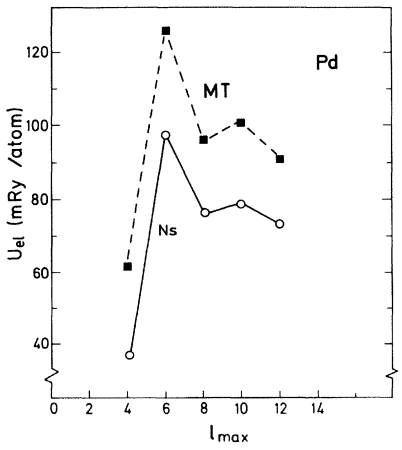

FIG. 6. Electrostatic energy (fcc Pd) calculated from Eq. (23). Dashed lines: muffin-tin charge density (MT). The interstitial density in this case is $\tilde{\rho}_0$ ($\tilde{\rho}_{\vec{G}}$ for $\vec{G}=\vec{0}$). Solid line: nonspherical charge (NS).

ACKNOWLEDGMENTS

The description of the nonsphericity in terms of the pseudo-MTO's and its continuation inside the spheres was suggested by O. K. Andersen. Furthermore, the author is grateful to him for several helpful discussions. W. Temmerman is thanked for help at the initial stages of the work, and the work would have been considerably more time consuming if the LMTO computer codes developed by D. Glötzel had not been available.

*Permanent address: Physics Laboratory I, The Technical University of Denmark, DK-2800 Lyngby, Denmark.

[1]O. K. Andersen, Phys. Rev. B 12, 3060 (1975).

[2]A. R. Mackintosh and O. K. Andersen, in *Electrons at the Fermi Surface,* edited by M. Springford (Cambridge Unversity Press, Cambridge, 1979).

[3]H. L. Skriver, in *The LMTO Method,* Vol. 41 of *Springer Series in Solid State Sciences* (Springer, New York, 1984).

[4]N. E. Christensen, Solid State Commun. 49, 701 (1984).

[5]O. K. Andersen (private communication).

[6]N. E. Christensen and D. Glötzel (unpublished).

[7]The nonspherical density inside the spheres can, of course, be determined directly from the LMTO eigenvectors and wave functions. An approximate way of doing this (Ref. 5) for the d states in transition metals is used in the elastic-constant calculations (Refs. 4 and 6). This leads to (Ref. 5) simple expressions for corrections to the multipole moments in terms of the differences in occupancies of E_g and T_{2g} states.

[8]O. Steinborn, Chem. Phys. Lett. 3, 671 (1969).

[9]S. Nagel, Phys. Rev. B 24, 4240 (1981).

[10]O. K. Andersen and R. G. Woolly, Mol. Phys. 26, 905 (1973).

[11]O. Jepsen and O. K. Andersen, Solid State Commun. 9, 1763 (1971), and D. Glötzel (private communication).

[12]N. E. Christensen (unpublished).